

Analysis of Heat Waves in Iran: Patterns, Trends, and Characteristics in Frequency, Intensity, and Duration (1980-2024)

Abbas Ranjbar Saadat Abadi¹, Amin Fazl Kazemi², Nasim Hossein Hamzeh³

1. Faculty member of Atmospheric Science and Meteorological Research Center, Tehran, Iran
2. Ph.D. Student of Meteorology, Institute of Geophysics, University of Tehran, Tehran, Iran
aminfazlkazemi@gmail.com
3. Department Meteorology, Air and Climate Technology Company (ACTC), Tehran, Iran.
nasim_hh@yahoo.com

Abstract

The increasing frequency and intensity of heat waves represent a pressing climate challenge globally. This study examines the patterns, trends, and characteristics of heat waves across 178 synoptic meteorological stations in Iran from 1980 to October 2024. Utilizing the Heat Wave Magnitude Index (HWMI), defined as periods where daily maximum temperatures exceed a specified threshold for three consecutive days, we observed a dramatic rise in heat wave occurrences—112.4%, 161.6%, and 391.1% in the second, third, and fourth decades compared to the first (1985-1994). Annually, approximately 28 heat waves were recorded, with an average magnitude of 6.4 and a duration of 23.8 days, particularly prevalent in the mountainous regions of the Zagros and Alborz ranges. This rise in heat waves in mountainous areas during colder seasons may be linked to feedback from reduced snow cover. The most severe heat wave occurred in summer 2024, marked by significant atmospheric features such as the clockwise rotation of the upper subtropical high's ridge line and intensified thermal low pressure in central Iran. These findings highlight the urgent need for adaptive resource management and climate resilience strategies. Policymakers should prioritize improved monitoring and predictive modeling to prepare communities for the growing impacts of extreme weather events, ensuring effective responses to the challenges posed by heat waves in Iran.

Keywords: Heat waves, Heat Wave Magnitude Index (HWMI), Meteorological analysis, Iran

1. Introduction

Since the 1950s, significant climate changes have occurred globally, with temperatures increasing by 1.4 degrees Celsius from 2013 to 2022, projected to rise by an additional 0.4 to 3.1 degrees Celsius by 2100 (Masson-Delmotte et al., 2021). Greenhouse gas emissions have led to increased frequency and intensity of weather hazards, particularly temperature extremes, with heat waves being the most likely to occur (Seneviratne et al., 2021). A heatwave is defined as a prolonged period of significantly elevated temperatures, typically lasting from several days to weeks. These extreme weather events pose serious health risks, particularly for vulnerable populations such as the elderly and those with preexisting conditions, and can lead to substantial economic and environmental challenges (Campbell et al. 2018). Heatwaves are often linked to unusual atmospheric circulation patterns. For example, during the North American heatwave in June 2021, a blocking high-pressure system in the upper troposphere led to the stagnation of warm air (Neal et al., 2022). Furthermore, changes in temperature thresholds are becoming increasingly pronounced, outpacing the effects of global warming, and forecasts indicate a rise in both the

frequency and intensity of heatwaves in the future (Intergovernmental Panel on Climate Change, 2012; Rahmstorf and Coumou, 2011).

Research has indicated that the increase in heat waves across the European Union and the UK is quite significant, particularly in southern European nations. Under the EU Reference socio-economic scenario from the 2015 Ageing Report, a 3 °C rise compared to pre-industrial levels could cause a heat wave currently occurring once every 50 years to happen almost annually in Spain and parts of Portugal, every three years in most southern regions, and at least once every five years in other areas of Europe (Naumann et al., 2020). Additionally, they assessed the impact of heat and cold extremes on the projected EU population for 2050 and 2100. As a 3°C warming scenario is unrealistic by mid-century, we focus on the Paris Agreement targets for 2050, assuming unchanged mortality rates based on recent disaster loss records. Smid et al. (2019) estimated the increased likelihood of heat waves for 31 European capitals (the capitals of 28 EU countries before 2020, plus Moscow, Russia; Oslo, Norway; and Zurich, Switzerland) and found that all examined European urban areas will be more exposed to extreme heat and heat waves in the coming decades.

In many regions of the world, temperature records have been broken, which can have severe impacts on the environment and society (McKinnon et al., 2022; Emerton et al., 2022; Thompson et al., 2022). The consequences of both rising average temperatures and the projected increase in frequency, intensity and duration of heat waves are concerning for public health. Globally, under a high warming scenario (Representative Concentration Pathway (RCP) 8.5), which is increasingly likely, every second summer will be as warm as the hottest summer experienced by the population from 1920 to 2014 (Lehner et al., 2018).

Heat waves have economic consequences, such as reduced productivity and increased energy consumption (Kjellstrom et al., 2016; García-León et al., 2021). Alizadeh et al. (2022) showed that observed trends in heat waves over the past four decades have been more pronounced in the lowest income quartile of the world than in other regions, leading to over a 40% increase in exposure from 2010 to 2019 compared to the highest income quartile. Lower-income regions have less adaptive capacity to warming, exacerbating the impacts of increased exposure to heat waves.

Zhao et al. (2024) predicted global, regional, and national mortality burdens related to heat waves for each grid cell (0.5°×0.5°) worldwide from 1990 to 2019 using a three-stage modeling framework. They found that during the warm seasons from 1990 to 2019, 153,078 deaths were associated with heat waves (nearly half in Asia), accounting for 0.94% of total deaths, equivalent to 236 deaths per 10 million people. Heat waves are deadly, but identifying these waves and better preparation can save lives (Harrington and Otto, 2020; Bittner et al., 2014). Preventive programs in response to weather hazards, including heat waves and urban heat, which involve measures such as establishing cooling centers or reducing working hours for outdoor workers, can mitigate the impacts of heat. For example, policy changes following the European heat wave in 2003 led to reduced mortality after a similar event in 2006 (Thompson et al., 2023).

Heat waves can be initiated and sustained by a variety of mechanisms, with critical factors closely associated with high-pressure ridges and positive geopotential height anomalies at the 500 hPa level. These phenomena are driven by the northward displacement of anticyclonic ridges, coupled with lower tropospheric temperature anomalies. Additionally, the presence of a dominant positive center characterized by descending motion across the research area further intensifies these conditions (Tomczyk et al., 2017; Agel et al., 2021; Qian et al., 2024).

The weakening of the polar jet stream due to global warming may be a possible reason for the increased likelihood of static weather patterns, leading to heavy precipitation or heat waves (Broennimann et al., 2009; Coumou et al., 2015; Mann, 2019).

To date, several climate indices have been used to quantify the intensity and duration of heat waves based on nighttime minimums or daily maximums (Perkins and Alexander, 2012; Frich et al., 2002; Schär et al., 2004; Fischer and Schär, 2010; Alexander et al., 2006; Orłowsky and Seneviratne, 2011; Russo and Sterl,

2011; Sillmann et al., 2013). However, all these indices have significant limitations when comparing the intensity of heat waves across different regions and times (Otto et al., 2012; Perkins and Alexander, 2012). Most defined indices for heat waves are generally considered with a specific group or section of impacts (such as human health, wildlife, agriculture, fire, management, transportation, and electricity) and due to their difficulty may not be transferable across different regions, among groups, or over different time periods (Perkins and Alexander, 2012). The heat wave duration index defined by Frich et al. (2002), which is one of the first proposed indices for identifying the impacts of heat waves, is statistically unstable (Kiktev et al., 2003; Alexander et al., 2006; Russo and Sterl, 2011).

In Iran, research on heat waves has revealed diverse trends, with many studies concentrating on specific provinces or limited timeframes. Notable works include Ghasemi et al. (2024), Sadeghi et al. (2015), Kashki et al. (2019), Almasi et al. (2016), Dargahian et al. (2021).

Barati and Mousavi (2005) examined heat waves in the cold season (from November to May) and concluded that the most heat waves manifest in the mountainous axes of the Zagros and Alborz ranges. Alijani and Farajzadeh (2015) studied the heat waves in northwestern Iran considering a fixed index, such as a daily maximum temperature of 40°C. Abbasnia et al. (2016) found that heat waves, unlike cold waves, have lengthened over the past three decades, concluding that the average intensity of heat waves in summer has increased by 3 to 4 degrees Celsius, with the most severe heat waves occurring in summer and spring along the southern coast of Iran, and the highest frequency observed in the Zagros Mountains and scattered heights in eastern Iran. During the period 1991-2013, heat waves showed an upward trend at all meteorological stations in the country, with the longest seasonal heat waves lasting approximately 10 to 16 days occurring in southeastern Iran (Yazdanpanah et al., 2017). Etemadian et al. (2021) concluded that most heat waves in Iran occurred in the western half and decreased towards the east, showing an upward trend in all months, with the significant difference being that the significance of the cold season months was higher than that of the warm period. Baharvandi et al. (2020) identified heat waves and analyzed their temporal and spatial changes during the period 1985-2015 based on daily maximum temperatures from 44 meteorological stations, showing that the most heat waves occur in the western part of the Zagros Mountain range. These studies contribute valuable insights but often lack a comprehensive national perspective, highlighting the need for broader analyses that encompass the entirety of Iran's climatic variability.

According to recorded statistics from the country's meteorological stations, over the past fifty years, the average temperature in the country has increased between 0.9 to 1.1 degrees Celsius, and during this time, various regions of the country have been affected by extreme temperatures and heat waves with varying intensity and frequency. However, in August 2024, the extent, intensity, and duration of the heat wave were unprecedented, causing the country to face challenges in providing sufficient electricity for cooling needs. Despite overall warming, the intensity and frequency of heat waves are changing across different spatial patterns.

In this study, we examine recorded heat waves at 178 meteorological stations over a period of more than 44.5 years, from 1980 to October 2024. Unlike previous studies in Iran, which often focus on specific provinces or case studies with limited temporal scope and few meteorological stations, our research offers a comprehensive national perspective. For a more precise analysis, in addition to determining the daily threshold wave, the 90th percentile temperature for each specific day in this period has been considered. To determine this percentile, 30 periods of 31 days centered on the same day in the reference climatic period (1991-2020) were selected from each station, and then a normal probability function was fitted to these 930 days. The 90th percentile of this function is defined as the threshold for the beginning and end of heat waves. Furthermore, we analyze the frequency, intensity, and duration of heat waves using a magnitude index, alongside investigating the atmospheric patterns associated with the most significant heat wave events in the country. This comprehensive data analysis, combined with our focus on Iran's diverse climatic regions and seasonal and annual trends, enhances the applicability of our findings to current global climate challenges. By addressing these critical issues, our study contributes to a deeper understanding of climatic patterns and improves future predictions.

2. Data and Research Methodology

In this study, the Heat Wave Magnitude Index (HWMI) is determined based on the method defined by Russo et al. (2014). In this method, the HWMI is defined as the maximum intensity of heat waves in a year, where a heat wave is referred to as a period of three consecutive days or more with daily maximum temperatures exceeding the daily threshold for the reference period of 1991–2020. The threshold is defined as the 90th percentile of daily maximum temperatures, based on a focused 31-day range (15 days before and 15 days after the specified day). Thus, for a specific day (d), the 90th percentile threshold from the dataset A_d is defined as follows (Russo et al., 2014):

$$A_d = U_{y=1991}^{2020} U_{i=d-15}^{d+15} T_{y,i} \quad (1)$$

where U represents the dataset, and $T_{y,i}$ is the maximum temperature on day i in year (y).

The criteria for defining a heat wave, particularly the minimum number of consecutive warm days, can differ significantly across various regions. For instance, Russo et al. (2015) and Perkins and Alexander (2012) characterize a heat wave as a global phenomenon that lasts for at least three consecutive days above a specified temperature threshold. In contrast, Fischer and Schär (2010) define a heat wave in Europe as an event persisting for a minimum of six days.

This difference in definitions is important; a six-day criterion would exclude shorter heat waves from consideration, while a three-day definition allows for the detection of extended heat events. In this study, we analyzed daily maximum temperature data from 178 meteorological stations covering the period from 1980 until the end of October 2024 (see Figure 1).

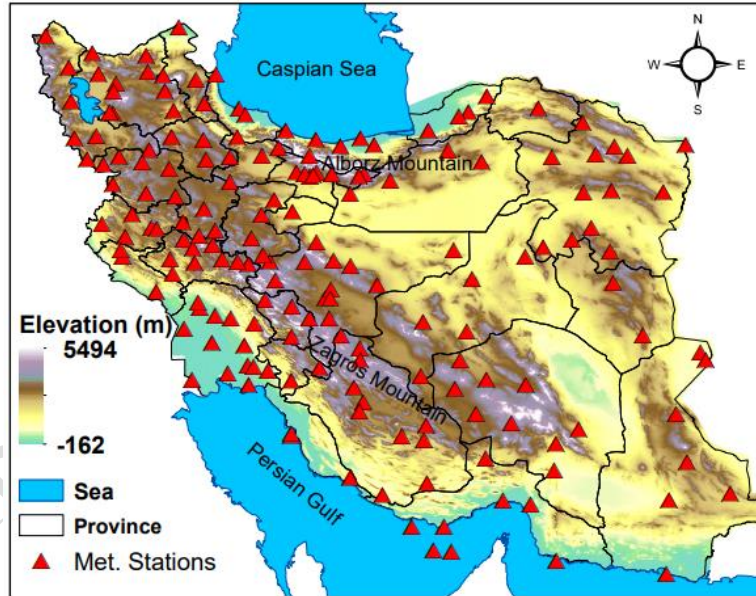


Figure 1: Location of the studied stations and the topography of the country

Following the selection of the stations, we applied the methodology outlined by Russo et al. (2014) to investigate the Heat Wave Magnitude Index (HWMI), along with the annual persistence, frequency,

intensity, and duration of heat waves at each station. The examination of heat wave persistence and frequency involved several systematic steps:

1. Establishing daily temperature thresholds: The daily threshold for identifying heat waves was determined by calculating the 90th percentile of temperatures for each day throughout the study period. This was achieved by selecting 30 distinct 31-day periods centered on each day from the reference climate period at each station. A normal probability function was fitted to these 930 days, with the 90th percentile serving as the threshold for initiating and concluding heat waves.
2. Identifying Heat Waves: For each year, we identified all heat waves defined as sequences of at least three consecutive days where daily maximum temperatures exceeded the established threshold.
3. Decomposing into Sub-Heat Waves: Each identified heat wave was segmented into sub-heat waves, where a sub-heat wave is defined as lasting three consecutive days. If a heat wave's total duration is not a multiple of three, the last one or two days are combined with preceding days to form a complete sub-heat wave.
4. Calculating Non-Scaled Magnitude of Sub-Heat Waves: The magnitude of a sub-heat wave is quantified as the sum of the daily maximum temperatures over the three-day period.
5. Normalizing the Magnitude of Sub-Heat Waves: This non-scaled magnitude is then transformed into a probability value ranging from 0 to 1, representing the normalized value of the sub-heat wave.
6. Aggregating Heat Wave Magnitudes: The overall magnitude of each heat wave is computed as the total of the magnitudes from all sub-heat waves.
7. Computing the Heat Wave Magnitude Index (HWMI): Finally, the HWMI for a given year is determined by taking the maximum magnitude among all recorded heat waves.

In this research, we implemented the aforementioned algorithm to analyze the annual maximum temperature data, summing the maximum temperatures of three consecutive days during heat wave events (non-scaled heat wave magnitude) from 1980 to October 2024.

After determining the probability function (supplementary A) corresponding to the unscaled values of the heat wave intensity (the sum of three consecutive maximum temperatures) and after separating each heat wave into several three-day periods (where at least one day from the heat wave and a maximum of two days after its conclusion are included in the last period), the unscaled values of heat wave intensity, after passing through the cumulative probability function, are converted into scaled values. Finally, after summing them in each continuous heat wave period, they represent the HWMI. The most intense heat wave in each year (or each season of each year separately) is considered the HWMI for each station and each year.

In some years, there may be more than one heat wave of varying magnitudes occurring at several stations. The heat wave with the highest intensity (magnitude) in each year is considered the annual heat wave (HWMI). In this study, while examining the length and intensity of annual heat waves at each station, the magnitude and persistence of all occurring waves have also been analyzed. Therefore, considering the above points, this study identifies and examines the number of heat waves and the total magnitude of annual heat waves over the past four decades (1984-2023), the number of seasonal and annual heat waves, the magnitude of all heat waves, the average duration of the largest annual heat wave, and the average annual duration of all heat waves over the 44-year period (1980-2023) and the first ten months of 2024 at 178 meteorological stations.

3. Results and Discussion

This section discusses the annual and seasonal distribution of heat waves, focusing on their frequency, intensity, and duration.

3.1. Annual Analysis

Over the past four decades (1984-2023), a total of 24,178 heat waves were recorded across 178 meteorological stations in Iran. Each decade has shown a marked increase in occurrences compared to the first decade (Figure 2). Specifically, the percentage changes in occurrences for the second (1994-2003), third (2004-2013), and fourth (2014-2023) decades relative to the first decade (1984-1993) were 112.4%, 161.6%, and 391.1%, respectively. Similarly, the average annual magnitude of heat waves increased significantly, with changes of 119.5%, 162%, and 280.1% across the same decades. The duration of heat waves also exhibited a notable upward trend, with increases of 55.1%, 70.9%, and 92.6%.

The average number of occurrences, duration and intensity of heat waves at the country's stations over these four decades is illustrated in Figure 2. Notably, the average duration and intensity of heat waves rose from 0.6 days and 6.7 in the first decade to 1.4 days and 22 in the fourth decade.

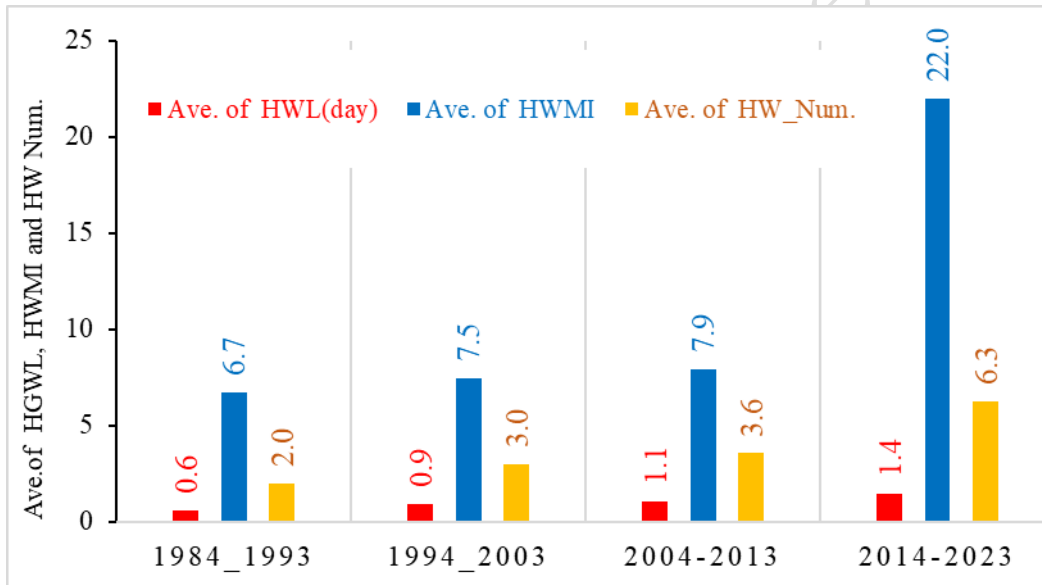


Figure 2. Average number of heat waves that occurred, annual magnitude of heat waves (HWMI), and their length (HWL) over the past four decades.

Figure 3 shows the total annual heat wave magnitudes (Figure 3-a), the total magnitudes of all heat waves (Figure 3-b), the average duration of annual heat waves (Figure 3-c), and the average duration of all heat waves (Figure 3-d) during the study period.

The total annual heat wave magnitude (Figure 3-a), which reflects the largest heat waves occurring in each region, indicates that in the eastern regions, the southern Zagros range (the heights of Kerman province and eastern Fars province), the west, northwest, central Alborz heights, and the southern shores of the Caspian Sea, the total magnitudes of heat waves (intensity of severe waves) have been the highest. Accordingly, during this time, the intensity of severe heat waves in vast areas of the Zagros and Alborz ranges has been significant. The range of variations was from 21.1 to 60.2, with maximum values of 60.2, 60.1, 59, and 53.1 occurring in Chaharmahal and Bakhtiari, Gilan, Fars, and Kerman provinces, respectively.

The range of variations in the total magnitudes of all heat waves that occurred in different regions of the country during the study period varied from 35 to 148, with maximum values observed in Gilan, Kermanshah, Chaharmahal and Bakhtiari, West Azerbaijan, Isfahan, Ilam, East Azerbaijan, and Kurdistan

provinces. Overall, the largest values (fourth quartile) of the total magnitudes of heat waves were often observed in the western regions and central Zagros heights (Figure 3-b).

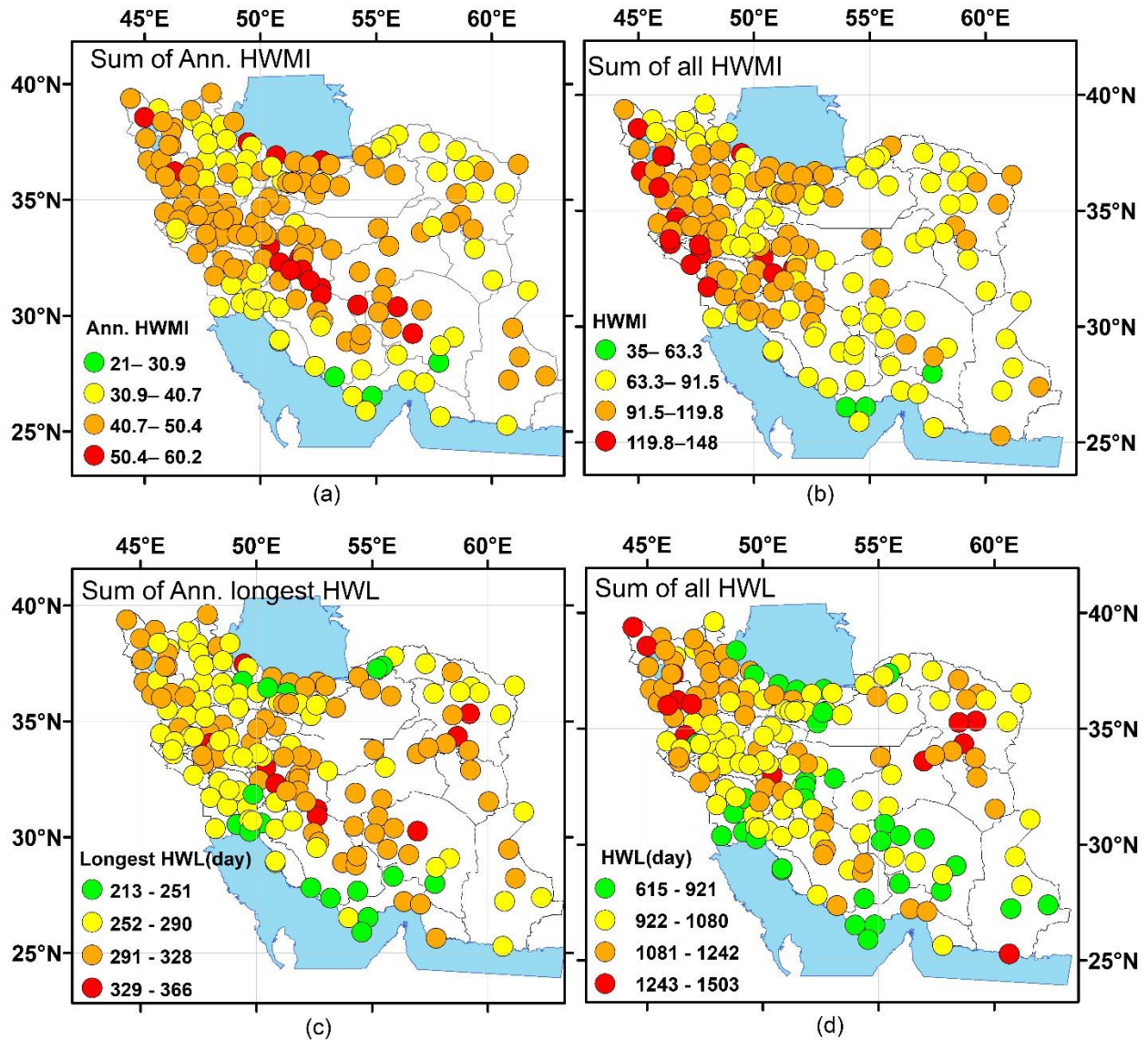


Figure 3. (a) total annual heat wave magnitudes, (b) total magnitudes of all heat waves, (c) total durations of annual heat waves, and (d) total durations of all heat waves during the study period

The total duration of annual heat waves varied from 213 days to 366 days. The longest durations of these waves occurred in regions within the Zagros and Alborz mountain ranges and eastern parts of the country, especially in the northeastern sections (Figure 3-c). Additionally, the total duration of all heat waves indicates that the persistence of heat waves has been notable in the northwestern and northeastern regions of the country (Figure 3-d). The average magnitude and duration of annual heat waves, including zero values, at meteorological stations during the study period (not shown in the figure) varied from 1.46 to 1.34 for the average magnitude of annual heat waves and from 4.73 days to 8.13 days for their average duration.

The annual total changes in the number, duration, and magnitude of heat waves in the country and their trends are shown in Figure 4. The annual trends of total heat wave magnitudes (red graph), their duration (blue graph), and the total number of heat waves (green graph) were 6.43, 23.77 days, and 28 occurrences per year, respectively. All of these trends showed a significant upward trajectory.

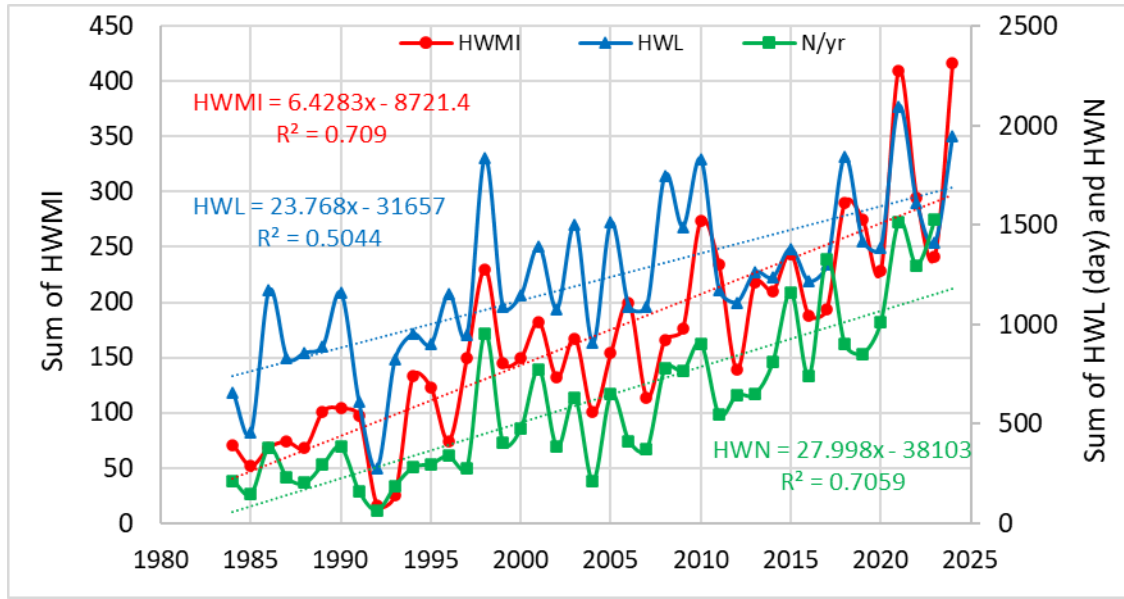


Figure 4. The trend of annual changes in frequency (green graph), length (blue graph) and magnitude of all heat waves (red graph) in Iran

3.2. Seasonal Analysis

Examining the spatial and seasonal distribution of heat waves is of great importance due to the serious impacts of this phenomenon. For instance, increased intensity and duration of these waves during the cold season can lead to snowmelt, increased flooding occurrences, and reduced water resource replenishment in the spring and summer seasons. In the warm season, in addition to the risks associated with heat stress, the demand for cooling significantly increases, challenging electricity supply capacity. Given the communities and resources at risk and the consequences of extreme weather events, such as heat waves, the timing and extent of the impact of these phenomena are crucial.

In this context, considering the spatial coverage of 178 meteorological stations, the annual and seasonal distributions of the number, intensity, and duration of these waves have been examined in two forms: one for annual heat waves magnitude (HWMI), which represents the largest heat wave in each year, and the other for all heat waves that occurred at each station.

For spatial distribution analysis, the total number of heat waves that occurred in various seasons during the study period (approximately 44.5 years, from 1980 to the end of October 2024) was identified and is displayed in Figure 5. The number of heat wave occurrences in different seasons is presented as quartiles with different colors (green, yellow, orange, and red, representing the first to fourth quartiles, respectively) in Figure 5.

During this period, the number of heat waves recorded in the spring ranged from 20 to 55, in the summer from 21 to 75, in the autumn from 8 to 48, and in the winter from 21 to 60 across various regions of the

country. In the spring, summer, and winter seasons, all regions of the country experienced at least 20 heat waves, with the highest number observed in the northwestern and northeastern areas and some southern regions. It is noteworthy that the number of stations in the third and fourth quartiles in the winter season, especially in cold regions such as the northwest, has significantly increased. The frequent occurrence of heat waves in winter in these areas can pose a serious threat to groundwater resource replenishment, snowmelt, and increased potential for flooding. This analysis indicates that a detailed examination of the spatial and seasonal distribution of heat waves can enhance understanding of their consequences and aid in planning for water and energy resource management.

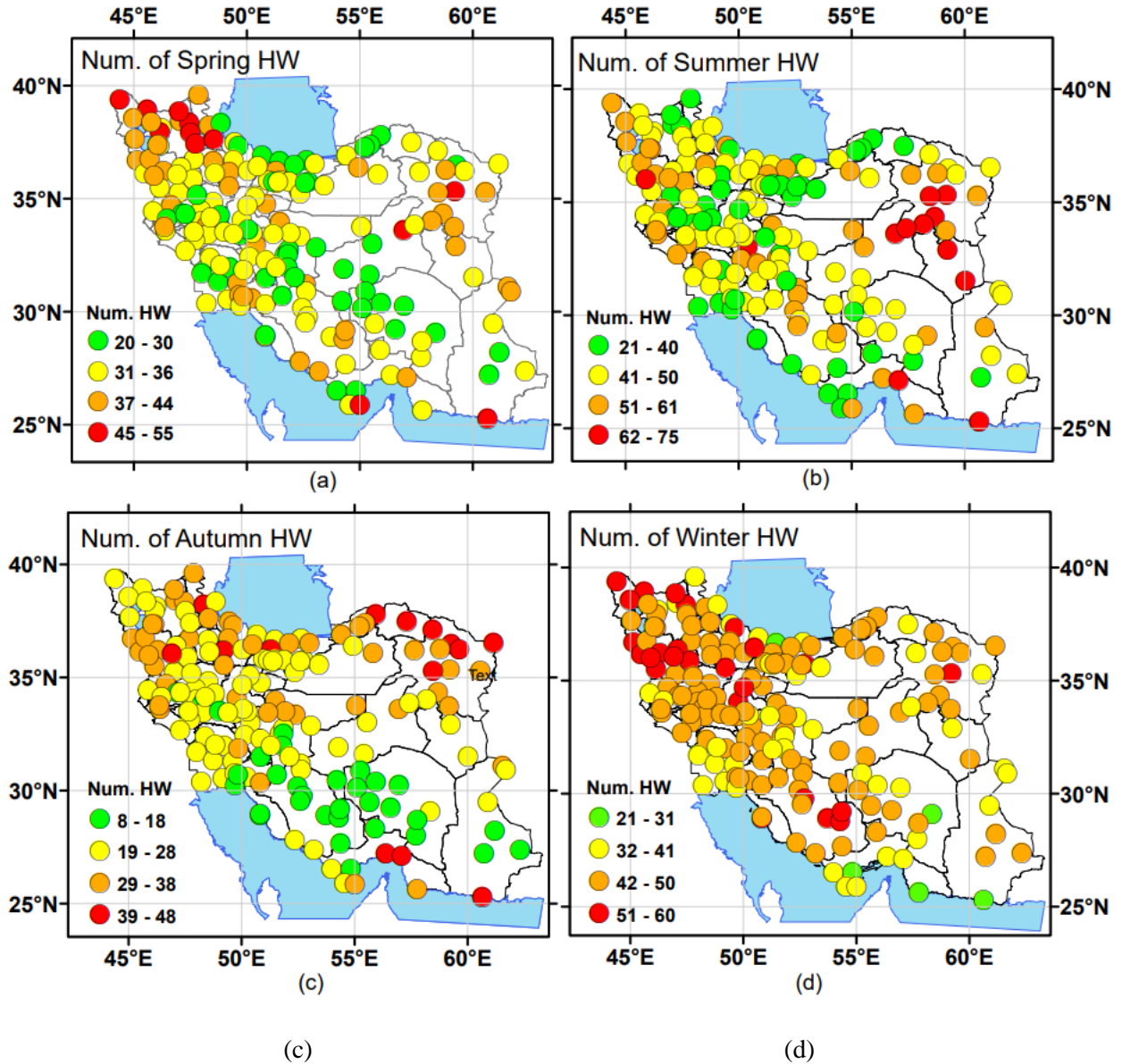


Figure 5. Number of heat waves occurred in seasons (a) spring, (b) summer, (c) autumn, and (d) winter during the study period (from 1980 to the End of October 2024)

The seasonal distribution of the total magnitudes of annual heat waves during the study period is shown in Figure 6, represented as quartiles of wave intensity. The range of seasonal intensity variations in spring, summer, autumn, and winter was between 15 to 41.7, 28.7 to 73.5, 3 to 30.3, and 2.7 to 4.4, respectively.

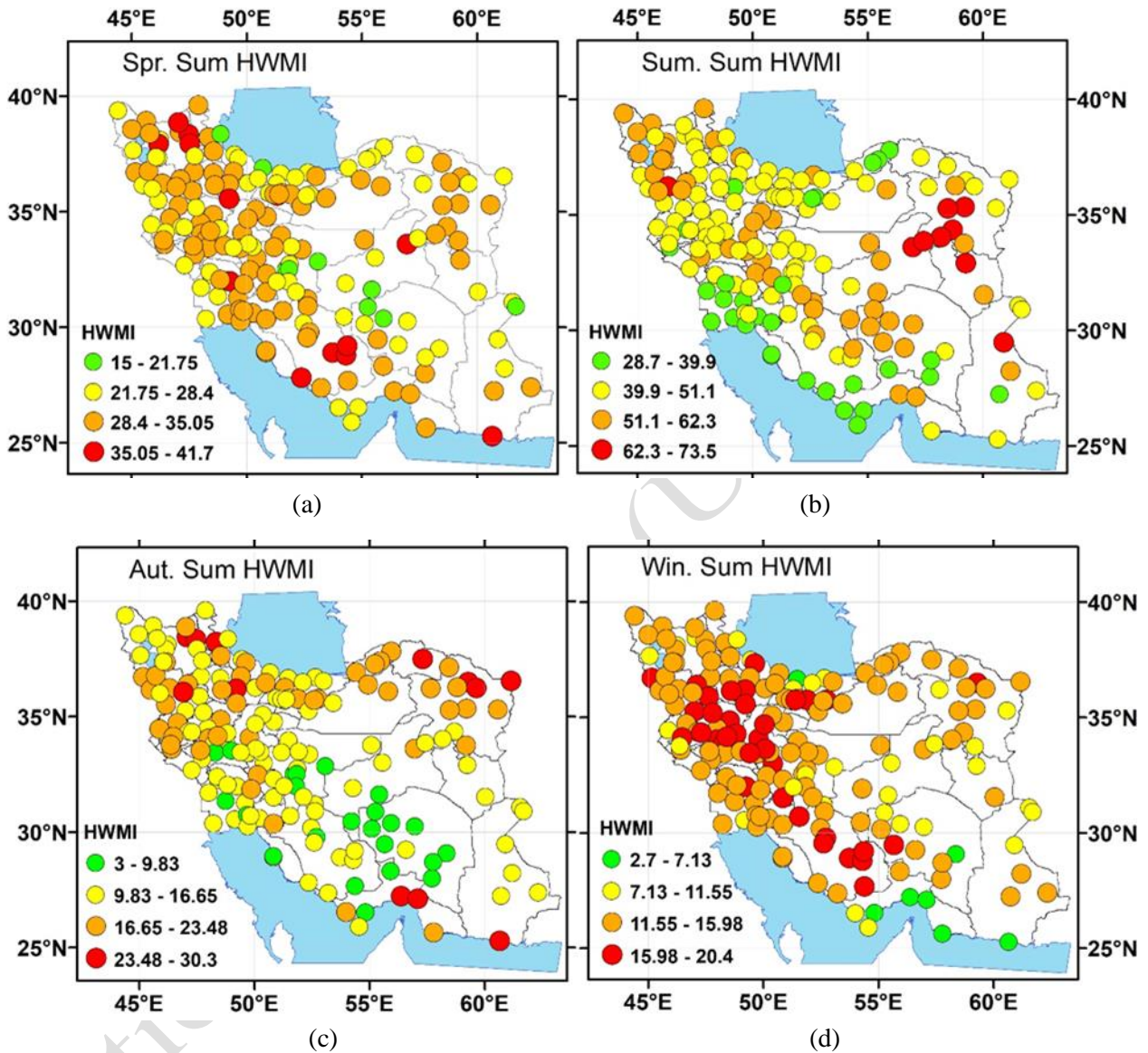


Figure 6. distribution of total annual heat wave magnitudes in seasons (a) spring, (b) summer, (c) autumn, and (d) winter during the study period

In spring and winter, heat waves with high intensities (third and fourth quartiles) predominated in most regions of the country (Figures 6-a & d), while extremely severe summer heat waves occurred in eastern regions, especially the northeast, with weaker intensity in the northwest of Kerman, eastern Fars, Qom, Markazi and areas around Lake Urmia (Figure 6-b).

In autumn, the highest intensity of heat waves was observed in the northeastern regions, parts of the northwestern and western country, and Hormozgan province (Figure 6-c). Severe heat waves in winter were widespread, affecting most regions of the country, especially the western areas during this time (Figure 6-

b). The consequences of severe heat wave occurrences in winter can be significant from various aspects, particularly in their role in snowmelt in colder regions.

The seasonal total of all heat wave magnitudes (Figure 7) indicates that the southwestern regions (especially Khuzestan province), western regions (especially Kermanshah, Hamadan, and West Azerbaijan provinces), and Tehran had the highest total intensities compared to other areas of the country in spring and winter (Figures 7-a & d). In summer, the highest intensities were observed in the western regions, northwest, southern Caspian Sea shores, and western parts of Isfahan province (Figure 7-b).

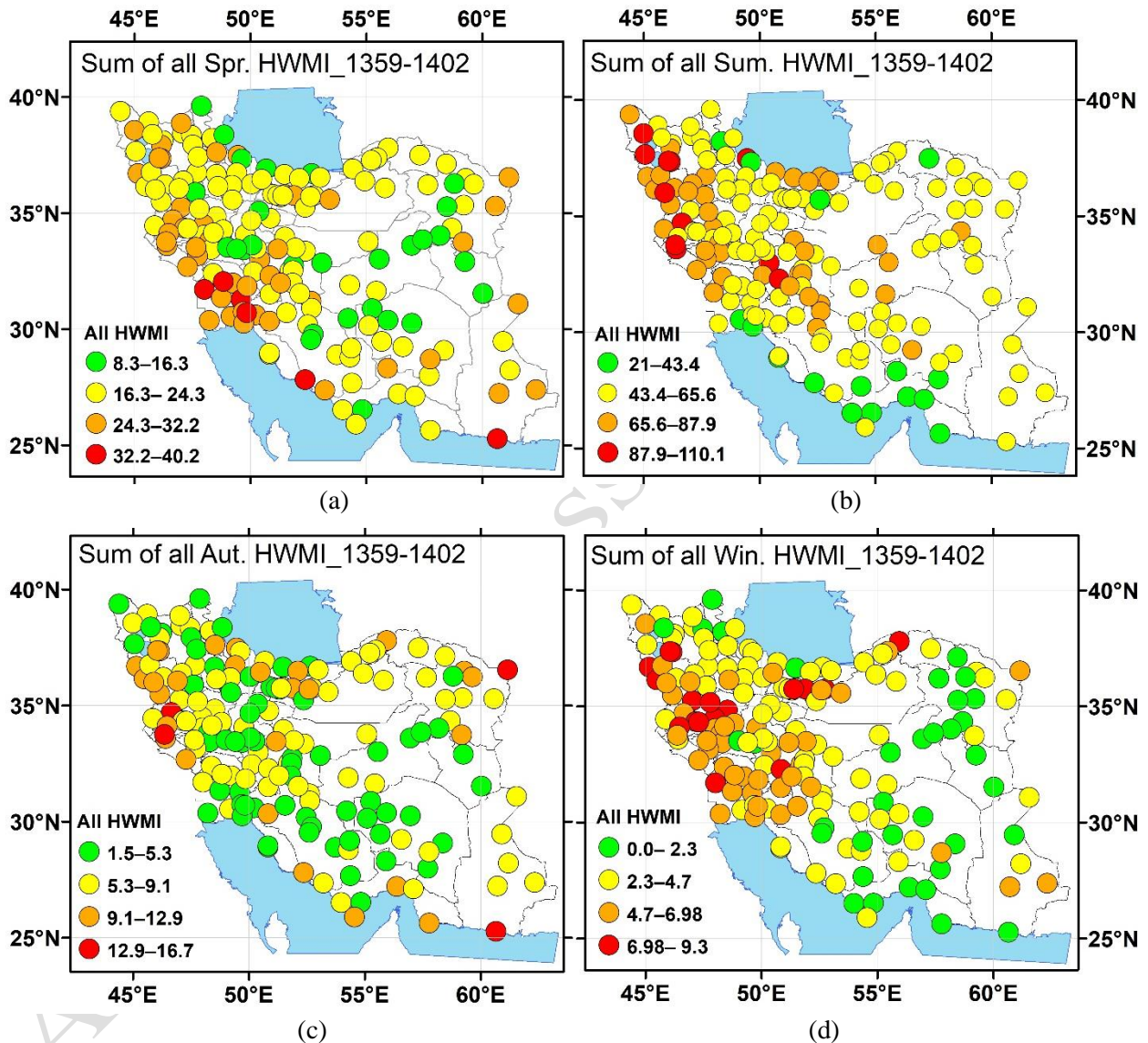


Figure 7. distribution of total magnitudes of all heat waves in seasons (a) spring, (b) summer, (c) autumn, and (d) winter during the study period

3.3 Iran's Record Heat Waves

The number of heat wave occurrences in Iran varied from 98 to 217 heat waves during the studied period (Figure 8-a). The third and fourth quartiles of this number were mostly related to the northeastern and northwestern regions of the country. Most of these areas are mountainous and have a temperate and cool climate, and the occurrence of the highest number of heat waves in these regions can have devastating

consequences for natural resources, especially pastures, forests, snow cover, water resources, and the agricultural sector.

From mid-March to mid-October 2024, approximately 760 heat waves were recorded across various weather stations, with an average duration of 7.4 days and an average intensity of 1.87. Notably, during the period from July 13 to August 24, 2024, 107 heat waves were documented, characterized by an average duration of 14.7 days and an intensity of 4.4. This timeframe marks the most prolonged and intense heat waves experienced in the country.

Throughout this period, heat waves impacted most regions of the country (see Figure 8-b) and shattered all previous records regarding both intensity and duration. When ranking heat waves by their intensity from highest to lowest, it is noteworthy that 27 out of the 50 most intense heat waves during the entire study period occurred in the summer of 2024.

To analyze the most severe heat waves during the study period, the heat waves were ranked according to their intensity, from highest to lowest magnitude. The top sixteen rankings of heat wave intensities were associated with provinces such as Isfahan, Yazd, Chaharmahal and Bakhtiari, Kerman, Sistan and Baluchestan, Fars, and South Khorasan. Notably, 12 of these heat waves occurred in August 2024 alone. The intensity and duration of these 16 heat waves exhibited considerable variation, with intensity levels ranging from 18.8 to 23.3 and durations spanning from 27 to 42 days.

The most severe heat waves were concentrated in the western and northwestern regions of Kerman, as well as in western Isfahan and Chaharmahal and Bakhtiari provinces (refer to Figure 8-b).

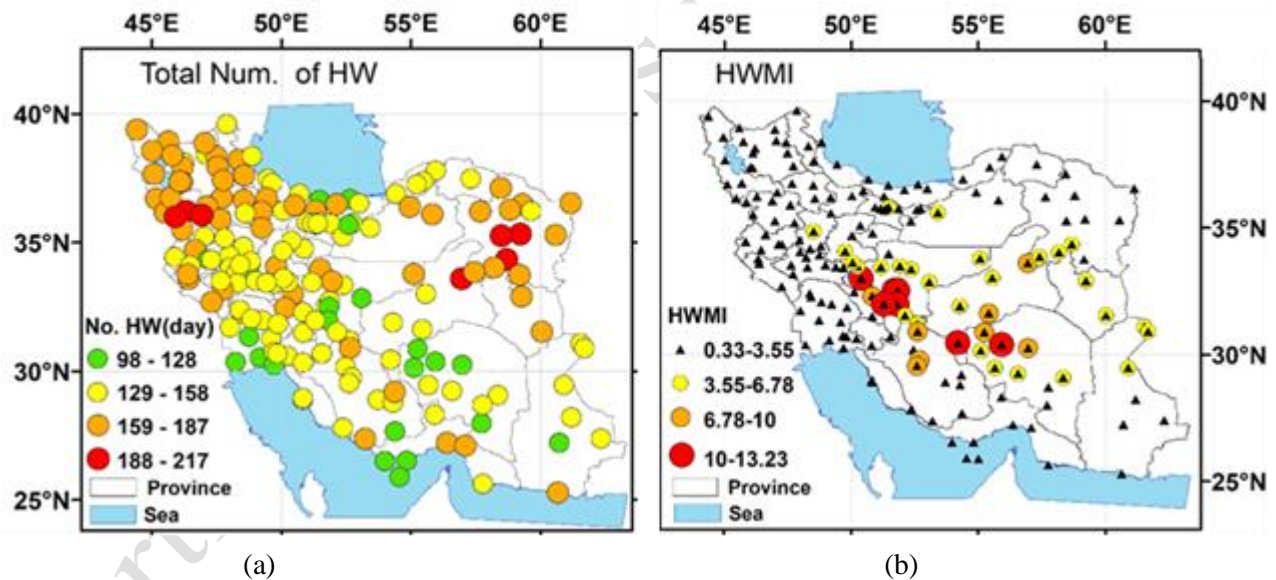


Figure 8. (a) number of heat waves during the entire study period, (b) intensity of heat waves in the spring and summer of 2024

3. 4 Synoptic Analysis of the Heat Wave Affecting Parts of the Country in July-August 2024

Temperature variations are primarily influenced by the solar declination angle and the heat capacity of the Earth's surface. Approximately 90% of the solar energy emitted reaches the Earth's surface, with about 51% of this energy being absorbed. This absorbed energy is not uniformly distributed, as it varies based on the

type, nature, and heat capacity of the surface, leading to thermal contrasts that result in temperature differences across various regions and the formation of thermal circulations.

During the summer months, the sun's rays strike the subtropical regions of the Northern Hemisphere nearly vertically, resulting in maximum thermal energy absorption and subsequent temperature increases. In late spring and summer, Iran (along with other subtropical arid regions) experiences a low-pressure thermal system due to significant solar energy absorption. This system typically originates over the Indian subcontinent, subsequently affecting parts of Pakistan and Iran, gradually penetrating from southeast Iran into desert areas and expanding northward.

The intensification of low-pressure systems, combined with subtropical high-pressure patterns, contributes to heat wave formation in summer observations reveal the establishment of a low-pressure thermal trough extending from central regions to the southeastern Caspian Sea, alongside a low-pressure system over the Persian Gulf, extending into Mesopotamia (Figure 9-a). Additionally, a low-pressure trough dominates Syria and the northeastern Mediterranean region. The presence of a trough at the 500 hPa level indicates the dynamic nature of this low-pressure system (Figure 9-b).

A high-pressure system situated between the Caspian Sea and the Black Sea extends its trough toward the eastern parts of the Zagros Mountains (Figure 9-a). Notably, there is a negative anomaly of approximately 3 to 4 millibars in sea level pressure during this period compared to the climatic baseline (1991-2020), indicating the strengthening of the low-pressure thermal system in central Iran. Furthermore, a significant negative pressure anomaly (exceeding 7 millibars) is observed over large areas north of the Caspian Sea and over Russia (Figure 9-a). These conditions correlate with severe negative anomalies in geopotential height at the 500 hPa (Figure 9-b), 850 hPa (Figure 9-c), and 700 hPa (Figure 9-d) levels.

At the 500 hPa level, a long-wave trough extends from the Black Sea to the Mediterranean, potentially generating weak waves in its eastern section that influence eastern regions. The upper-level ridge extending from North Africa into Iran has shifted its orientation from the typical south-north axis to a west-east alignment, a notable feature contributing to the occurrence of severe heat waves during this period. Additionally, a positive anomaly exceeding 30 meters at the 500 hPa level is observed over Iran (see Figure 9-b), indicating the strengthening of the subtropical high-pressure system.

At the 850 hPa level, a low-pressure system dominates over Pakistan and southern Iran, with a trough extending from Pakistan to the western Arabian Sea and eastern Arabia. An inverted low-pressure system in southern Iran extends into northern Iraq, continuing over Syria and the northern Mediterranean (see Figure 9-c). This is accompanied by the establishment of a ridge in the northern part of the trough, extending northeastward into Iran and creating a high-pressure system with a central height of 150 decameters over the eastern Caspian Sea.

The average geopotential height during the climatic period from July 13 to August 24, as indicated by the dashed black contours at the 500 hPa (Figure 9-b) and 700 hPa levels (Figure 9-d), shows that the upper-level high of the subtropical zone extends from the Persian Gulf to the central regions of Russia. However, during the period from July 13 to August 2024, this upper-level high expansion to northern latitudes is significantly limited. This limitation is primarily due to the presence of a strong tilting trough north of the Aral Lake and a long-wavelength trough over the Black Sea and eastern Mediterranean.

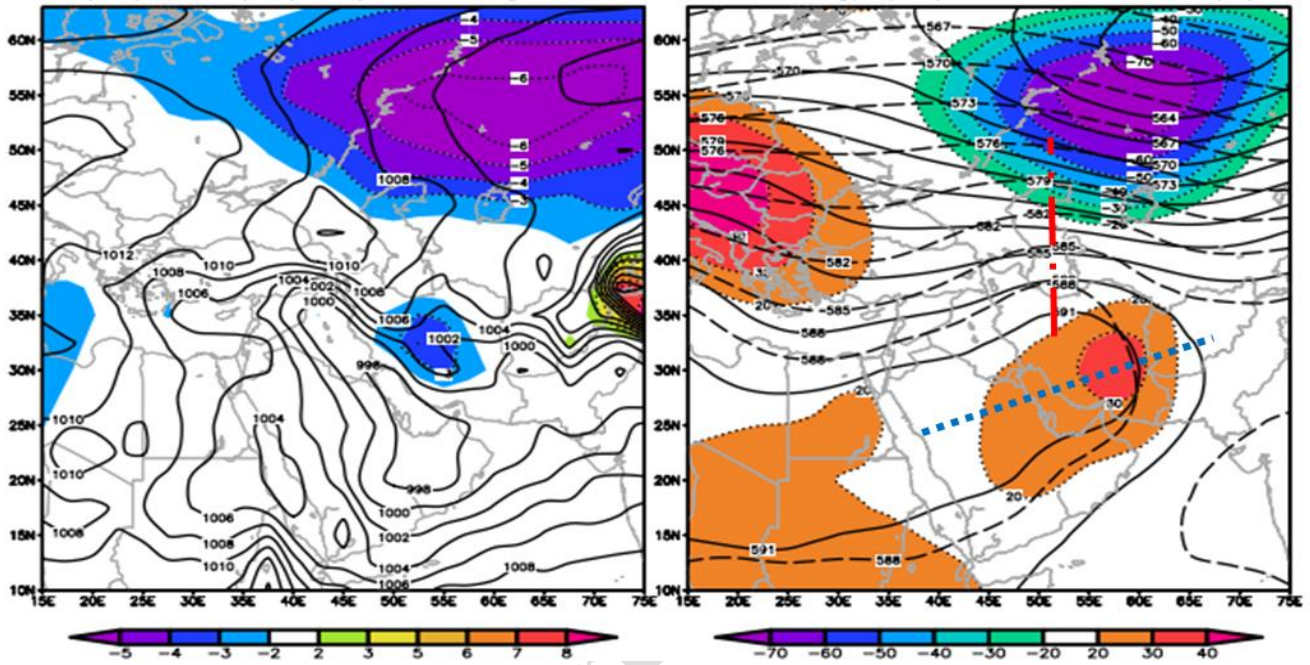
These atmospheric conditions have resulted in a significant shift of the upper ridge axis over Iran, which typically runs in a south-north orientation, to a southwest-northeast alignment during this period. This alteration, combined with other contributing factors, has led to the strengthening and persistence of heat-low pressure in the southern and central regions of Iran. Consequently, these conditions have given rise to unprecedented and prolonged heat waves in these areas.

The range of positive air temperature anomalies near the Earth's surface, at the 700 hPa and 600 hPa levels (Figure 10a), indicates extremely hot areas during the recent period. The extension of positive temperature anomalies up to approximately 600 hPa and higher signifies a substantial intensification of the heat-low

pressure, extending to altitudes exceeding around 4000 meters above sea level. The enhancement of the 200 hPa geopotential height by about 80 meters over Iran, along with the restricted northward expansion compared to the climatic period, is influenced by a low-pressure system located north of the Aral Sea (Figure 10b & c). A significant increase in jet streams positioned in the southern Alborz region (Figure 10d) suggests that the subtropical jet stream has not extended to higher latitudes, which is a consequence of the limited low heat pressure system in the southern regions.

SLP(mb)& Ano.(mb)_July 13, to Aug. 24 2004

500mb-gph(dm), Mean, Clim., & Ano.(m)



850mb-gph[dm]& Ano.(m)

700mb-gph(dm), Mean, Clim., & Ano.(m)

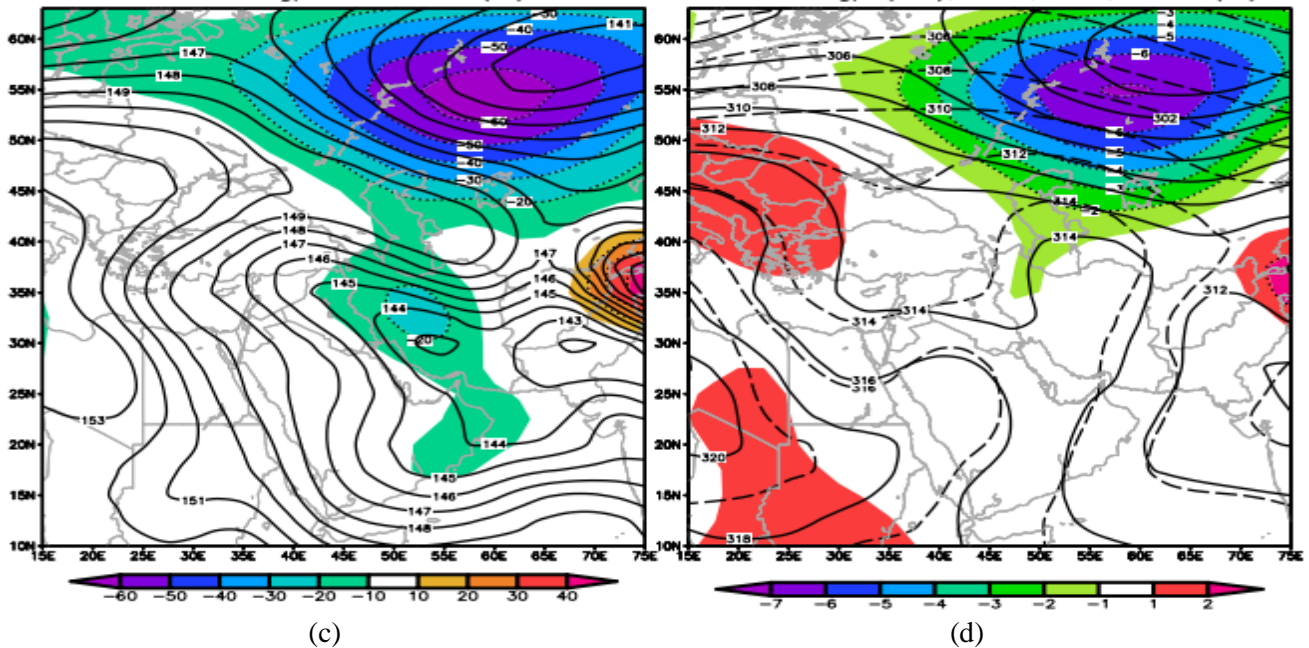


Figure 9. (a) Average sea level pressure from July 13 to August 24, 2024, along with its anomalies compared to the climatic baseline of 1991-2020. (b) Average geopotential height at the 500-hPa level during the same period, illustrated with solid black contours for the recent data and dashed black contours for the

corresponding climatic period. The shaded areas represent geopotential height anomalies for the recent period, while the ridge lines for the climatic period are indicated by red dashed lines and those for the recent period by blue dotted lines. (c) Average geopotential height at the 850-hPa level for the specified period, depicted with solid black contours, alongside their corresponding anomalies shown as shaded areas. (d) Average geopotential height at the 700-hPa level in the same timeframe, featuring solid black contours for the recent period and dashed black contours for the similar climatic period, with shaded areas representing the anomalies for the recent period.

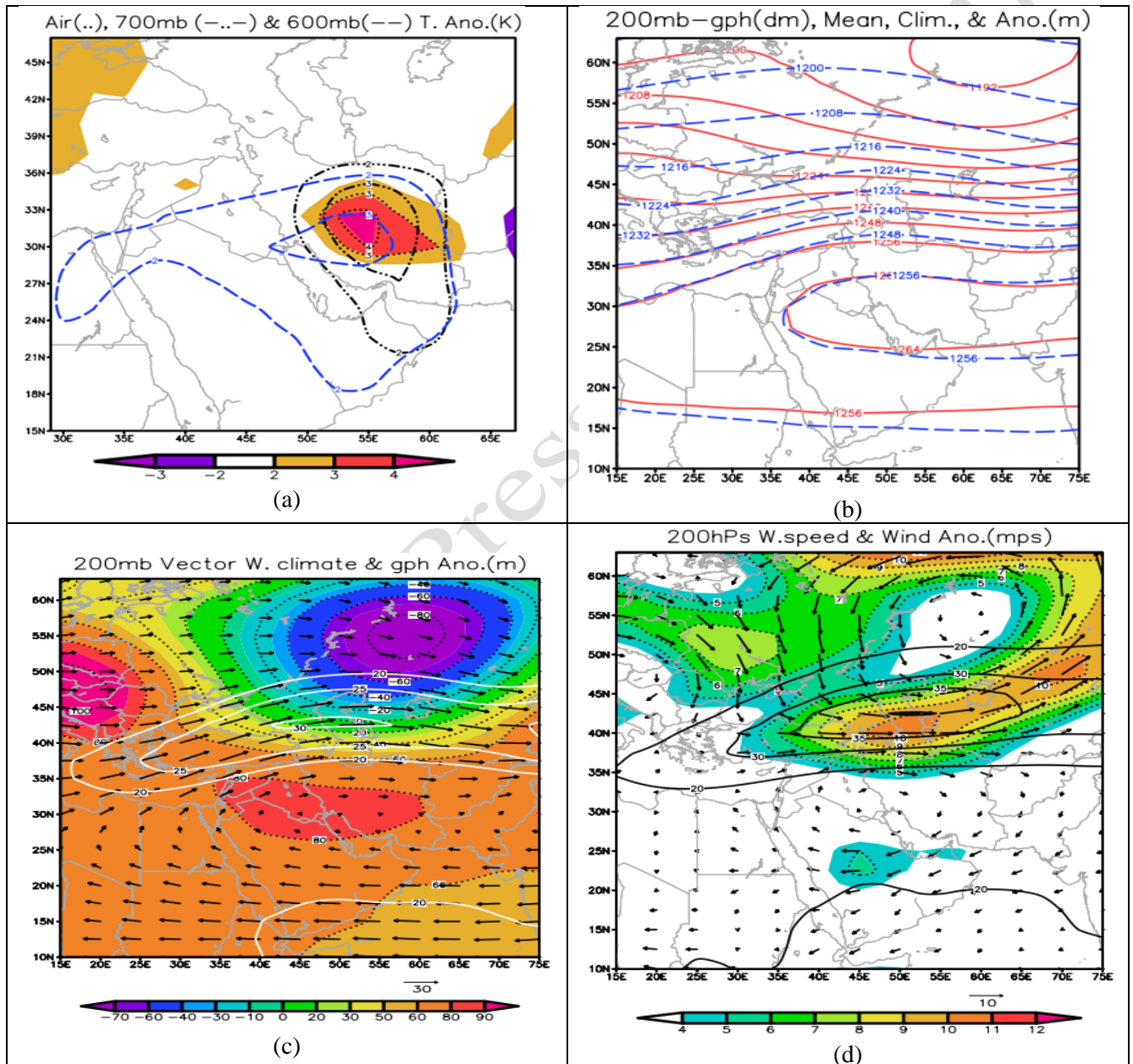


Figure 10. (a) Anomalies of near-surface air temperatures (shaded areas), 700 hPa level (black dashed lines), and 600 hPa surface temperatures compared to the similar climatic period. (b) Average geopotential height at the 200 hPa level during the recent period (red contours) and the comparable climatic period (blue dashed

contours). (c) Anomalies of geopotential height at the 200 hPa level during the recent period compared to the similar climatic period (shaded areas and black dot contours) and wind speed contours at the 200 hPa level for the climatic period (white contours). (d) Anomalies of wind vectors and wind speed (shaded area) at the 200 hPa level during the recent period compared to the climatic period, along with wind speed contours for this period.

3.5 Discussion

The analysis of heat waves in Iran from 1980 to 2024 reveals significant trends in frequency, intensity, and duration, with a total of 24,178 heat waves recorded across 178 meteorological stations. This study's findings align with previous research indicating a marked increase in heat wave occurrences over the past decades. For instance, studies by Ghasemi et al. (2024) and Sadeghi et al. (2015) have similarly reported that heat waves have become more prevalent, particularly in mountainous regions such as the Zagros and Alborz ranges.

The observed percentage changes in the occurrences of heat waves—112.4%, 161.6%, and 391.1% across successive decades—highlight the escalating intensity of this phenomenon. These findings align with the research conducted by Yazdanpanah et al. (2017), which identified a discernible upward trend in heat wave durations, particularly in southeastern Iran, where the longest events spanned between 10 and 16 days. Moreover, the analysis by Etemadian et al. (2021) reinforces the idea that the frequency of heat waves has risen across all months, with notable increases during the winter months compared to the summer.

The spatial and seasonal distribution of heat waves is critical for understanding their impacts. Our findings indicate that the northeastern and northwestern regions experience the highest occurrences, consistent with the research of Baharvand et al. (2020), which identified the western Zagros as a hotspot for heat wave activity. The implications of these findings are profound, particularly regarding water resource management and agricultural practices, as highlighted by the increased demand for cooling in urban areas during heat waves.

Moreover, the examination of heat wave magnitudes reveals that the most severe heat waves occurred in the eastern regions, particularly the southern Zagros and the Caspian Sea shores. This observation aligns with the work of Abbasnia et al. (2016), who found that the intensity of heat waves has increased by 3 to 4 degrees Celsius in recent decades, especially during summer and spring.

The persistence of heat waves, particularly in winter, poses additional challenges, as indicated by our results showing that regions typically not associated with high temperatures are now experiencing significant heat wave activity. This trend is alarming, as it can lead to adverse effects such as increased flooding and reduced groundwater replenishment, echoing the concerns raised by Dargahian et al. (2021) regarding the implications of winter heat waves on natural resources.

The atmospheric patterns influencing these heat waves are characterized by high-pressure ridges and positive geopotential height anomalies at the 500 hPa level. The northward displacement of anticyclonic ridges, combined with lower tropospheric temperature anomalies, creates conditions favorable for heat wave development. Additionally, the establishment of low-pressure thermal systems, particularly those originating over the Indian subcontinent, contributes significantly to the intensity and persistence of heat waves in Iran.

In conclusion, the findings of this study not only enhance our understanding of heat wave patterns in Iran but also highlight the urgent need for effective climate adaptation strategies. The significant upward trends in heat wave frequency and intensity necessitate a reevaluation of resource management policies to mitigate the impacts of this escalating climate phenomenon.

4. Conclusion

The findings of this study underscore a dramatic escalation in heat wave occurrences over the past four decades (1984-2023), revealing critical insights into the increasing frequency and intensity of these extreme weather events. Notably, the frequency surged from 2,270 in the first decade to 11,148 in the fourth decade,

marking an astonishing 391.1% increase. This upward trend is particularly pronounced in the second and third decades, which recorded percentage increases of 112.4% and 161.6%, respectively. Such figures not only reflect a growing prevalence of heat waves but also point to the urgent need for proactive measures to mitigate their impacts.

In addition to frequency, the average annual heat wave magnitude has undergone significant transformations during this timeframe. Specifically, the average annual magnitude rose by 119.5% in the second decade, 162% in the third decade, and a remarkable 280.1% in the fourth decade. These figures indicate that not only are heat waves occurring more frequently, but they are also becoming more intense and persistent, posing greater risks to many aspects, especially the environment.

Spatial distribution analysis reveals that the eastern regions, southern Zagros range, as well as the western, northwestern, and central Alborz heights, are experiencing the highest intensity of heat waves. In these areas, total magnitudes of annual heat waves varied between 21.1 and 60.2, with peak values recorded in provinces such as Chaharmahal and Bakhtiari, Gilan, Fars, and Kerman. Furthermore, the total duration of these annual heat waves ranged from 213 days to 366 days, with the longest durations observed in the Zagros and Alborz regions, as well as the eastern parts of the country.

The seasonal analysis indicates that heat waves are not confined to summer; significant occurrences were also noted during spring and winter. The range of changes in the total magnitudes of extreme heat waves across seasons varied considerably, with the highest intensities observed in summer, followed by spring. The increased intensity and duration of heat waves during the cold season are particularly concerning, as they may lead to accelerated snowmelt, heightened flooding occurrences, and diminished replenishment of water resources in the spring and summer months.

The implications of these changes during the cold season are particularly significant. The increased intensity and duration of heat waves may lead to accelerated snowmelt, heightened flooding occurrences, and diminished replenishment of water resources in the spring and summer months. The frequent occurrence of heat waves during winter in traditionally colder regions poses a severe threat to groundwater replenishment and escalates the risk of flooding.

Ultimately, this study highlights the urgent need for strategic planning and management of water and energy resources, especially in light of the challenges posed by climate change and the rising frequency of heat waves. A comprehensive examination of the spatial and seasonal distribution of these waves will enhance our understanding of their consequences and facilitate the implementation of effective measures to mitigate their adverse impacts.

Moreover, it is imperative for policymakers and stakeholders to consider these findings in their climate adaptation strategies, ensuring that infrastructure and resource management are equipped to handle the increasing pressures from extreme weather events. Enhanced monitoring and predictive modeling of heat waves can also play a crucial role in preparing communities for the potential impacts, ultimately contributing to greater resilience in the face of a changing climate.

References:

Abbasnia, M., Tavousi, T., Khosravi, M., & Toros, H. (2016). Spatial-temporal analysis of heat waves in Iran over the last three decades. *Natural Environment Change*, 2(1), 25-33. (In Persian).

Alexander, L. V., Zhang, X., Peterson, T. C., Caesar, J., Gleason, B., Tank, A., Haylock, M., Collins, D., Trewin, B., Rahimzadeh, F., Tagipour, A., Kumar, K. R., Revadekar, J., Griffiths, G., Vincent, L., Stephenson, D. B., Burn, J., Aguilar, E., Brunet, M., Taylor, M., et al. (2006). Global observed changes in daily climate extremes of temperature and precipitation. *Journal of Geophysical Research*, 111, D05109. <https://doi.org/10.1029/2005JD006290>

Alijani, B., & Farajzadeh, H. (2015). Analysis of trends in extreme temperature indices in northern Iran. *Geography and Planning*, 19(52), 229-256. (In Persian).

- Almasi, F., Tavousi, T., & Hosseinabadi, N. (2016). Analysis of the behavior and changes in the frequency of heat wave events in Ahvaz. *Journal of Geographic Space Studies*, 6(19), 135-150. (In Persian).
- Alizadeh, M. R., Abatzoglou, J. T., Adamowski, J. F., Prestemon, J. P., Chittoori, B., Akbari Asanjan, A., & Sadegh, M. (2022). Increasing heat-stress inequality in a warming climate. *Earth's Future*, 10, e2021EF002488. <https://doi.org/10.1029/2021EF002488>
- Agel, L., Barlow, M., Skinner, C., et al. (2021). Four distinct Northeast US heat wave circulation patterns and associated mechanisms, trends, and electric usage. *Nature Communications*, 4(1). <https://doi.org/10.1038/s41612-021-00186-7>
- Baharvandi, N., Mojared, F., & Masoumpour, J. (2020). Identification of heat waves and analysis of their temporal-spatial changes in Iran. *Journal of Applied Geographic Sciences*, 20(59), Winter 2020. (In Persian).
- Barati, G., & Mousavi, S. Sh. (2005). Spatial displacement of winter heat waves in Iran. *Journal of Geography and Development*, 5, 41-52. (In Persian).
- Bittner, M. I., Matthies, E. F., Dalbokova, D., & Menne, B. (2014). Are European countries prepared for the next big heat wave? *European Journal of Public Health*, 24, 615–619.
- Broennimann, S., Stickler, A., Griesser, T., Ewen, T., Grant, A. N., Fischer, A. M., Schraner, M., Peter, T., Rozanov, E., & Ross, T. (2009). Exceptional atmospheric circulation during the "Dust Bowl". *Geophysical Research Letters*, 36, L08802. <https://doi.org/10.1029/2009GL037612>
- Campbell, S., Remenyi, T. A., White, C. J., & Johnston, F. H. (2018). Heatwave and health impact research: A global review. *Health & Place*, 53, 210–218. <https://doi.org/10.1016/j.healthplace.2018.08.017>
- Coumou, D., Lehmann, J., & Beckmann, J. (2015). The weakening summer circulation in the Northern Hemisphere mid-latitudes. *Science*, 348, 324–327. <https://doi.org/10.1126/science.1261768>
- Dargahian, F., Heydarnajad, S., & Razavi Zadeh, S. (2021). Examining the trend of changes in heat wave characteristics related to climate change (Case study: Yazd County). *Scientific Journal of Research in Rangeland and Desert*, 28(3), 564-577.
- Emerton, R., Brimicombe, C., Magnusson, L., Roberts, C., Di Napoli, C., Cloke, H. L., & Pappenberger, F. (2022). Predicting the unprecedented: Forecasting the June 2021 Pacific Northwest heatwave. *Weather*, 77, 272–279.
- Etemadian, A., Doostan, R., & Zarrin, A. (2021). Heat wave regions in Iran. *Climatology Research*, 11(42). (In Persian).
- Fischer, E. M., & Schär, C. (2010). Consistent geographical patterns of changes in high-impact European heatwaves. *Nature Geoscience*, 3, 398–403. <https://doi.org/10.1038/NGEO866>
- Frich, P., Alexander, L. V., Della-Marta, P., Gleason, B., Haylock, M., Klein Tank, A., & Peterson, T. (2002). Global changes in climatic extremes during the second half of the 20th century. *Climate Research*, 19, 193–212.
- García-León, D., et al. (2021). Current and projected regional economic impacts of heatwaves in Europe. *Nature Communications*, 12(1). <https://doi.org/10.1038/s41467-021-26050-z>
- Ghasemi, M., Baqideh, M., & Entezari, M. (2024). Statistical study of heat wave characteristics in Isfahan Metropolis. *Journal of Environmental Science Studies*, 9(4), 9371-9357.
- Harrington, L. J., & Otto, F. E. L. (2020). Reconciling theory with the reality of African heatwaves. *Nature Climate Change*, 10, 796–798.
- Intergovernmental Panel on Climate Change. (2012). *Managing the risks of extreme events and disasters to advance climate change adaptation: A special report of Working Groups I and II of the Intergovernmental Panel on Climate Change* (C. B. Field et al., Eds.). Cambridge University Press.
- Kashki, A., Karami, M., Baqideh, M., & Alimoradi, M. (2019). Statistical analysis of heat waves in Zabol. *Journal of Climate Change and Environmental Hazards*, 1(1), Zanzan University, 40-55.
- Kiktev, D., Sexton, D. M. H., Alexander, L., & Folland, C. K. (2003). Comparison of modelled and observed trends in indices of daily climate extremes. *Journal of Climate*, 16, 3560–3571.

- Kjellstrom, T., et al. (2016). Heat, human performance, and occupational health: A key issue for the assessment of global climate change impacts. *Annual Review of Public Health*, 37(1), 97–112. <https://doi.org/10.1146/annurev-publhealth-032315-021740>
- Lehner, F., Deser, C., & Sanderson, B. M. (2018). Future risk of record-breaking summer temperatures and its mitigation. *Climate Change*, 146(3), 363–375. <https://doi.org/10.1007/s10584-016-1616-2>
- Mann, M. E. (2019). The weather amplifier: Strange waves in the jet stream foretell a future full of heat waves and floods. *Scientific American*, 320(3), 43–49.
- Masson-Delmotte, V., Zhai, P., Pirani, A., Connors, S., Péan, C., Berger, S., et al. (2021). *Climate Change 2021: The Physical Science Basis: Contribution of Working Group I to the Sixth Assessment Report of the Intergovernmental Panel on Climate Change*. Cambridge University Press.
- McKinnon, K. A., & Simpson, I. R. (2022). How unexpected was the 2021 Pacific Northwest heatwave? *Geophysical Research Letters*, 49, e2022GL100380.
- Naumann, G., Russo, S., Formetta, G., Ibarreta, D., Forzieri, G., Girardello, M., & Feyen, L. (2020). Global warming and human impacts of heat and cold extremes in the EU. EUR 29959 EN, Publications Office of the European Union, Luxembourg. <https://doi.org/10.2760/47878>, JRC118540
- Neal, E., Huang, C. S. Y., & Nakamura, N. (2022). The 2021 Pacific Northwest heat wave and associated blocking: Meteorology and the role of an upstream cyclone as a diabatic source of wave activity. *Geophysical Research Letters*, 49, e2021GL097699.
- Orlowsky, B., & Seneviratne, S. (2011). Global changes in extreme events: Regional and seasonal dimension. *Climate Change*, 110, 669–696.
- Otto, F. E. L., Massey, N., van Oldenborgh, G. J., Jones, R. G., & Allen, R. M. (2012). Reconciling two approaches to attribution of the 2010 Russian heat wave. *Geophysical Research Letters*, 39, L04702. <https://doi.org/10.1029/2011GL050422>
- Perkins, S. E., & Alexander, L. V. (2012). On the measurement of heat waves. *Journal of Climate*, 26, 4500–4517.
- Qian, Z., Sun, Y., Ma, Q., et al. (2024). Understanding changes in heat waves, droughts, and compound events in Yangtze River Valley and the corresponding atmospheric circulation patterns. *Climate Dynamics*, 62, 539–553. <https://doi.org/10.1007/s00382-023-06927-z>
- Rahmstorf, S., & Coumou, D. (2011). Increase of extreme events in a warming world. *Proceedings of the National Academy of Sciences USA*, 108, 17905–17909.
- Russo, S., & Sterl, A. (2011). Global changes in indices describing moderate temperature extremes from the daily output of a climate model. *Journal of Geophysical Research*, 116, D03104. <https://doi.org/10.1029/2010JD014727>
- Russo, S., Dosio, A., Graverson, R. G., Sillmann, J., Carrao, H., Dunbar, M. B., et al. (2014). Magnitude of extreme heat waves in present climate and their projection in a warming world. *Journal of Geophysical Research: Atmospheres*, 119, 12500–12512. <https://doi.org/10.1002/2014JD022098>
- Russo, S., Sillmann, J., & Fischer, E. M. (2015). Top ten European heatwaves since 1950 and their occurrence in the coming decades. *Environmental Research Letters*, 10(12), 124003. <https://doi.org/10.1088/1748-9326/10/12/124003>
- Sadeghi, S., Doostan, R., & Sanei, M. (2015). Temporal-spatial analysis of heat waves in Khorasan Razavi. *Geography Journal of the Land*, 12(47), 17-32.
- Schär, C., Vidale, P. L., Lüthi, D., Frei, C., Häberli, C., Liniger, M. A., & Appenzeller, C. (2004). The role of increasing temperature variability in European summer heatwaves. *Nature*, 427, 332–336.
- Seneviratne, S. I., Zhang, X., Adnan, M., Badi, W., Dereczynski, C., Di Luca, A., Ghosh, I., Iskandar, J., Kossin, S., Lewis, F., Otto, I., Pinto, M., Satoh, S. M., Vicente-Serrano, M., Wehner, B., & Zhou, B. (2021). Weather and climate extreme events in a changing climate. In *Climate Change 2021: The Physical Science Basis* (pp. 1513–1766). Cambridge University Press. <https://doi.org/10.1017/9781009157896.013>

- Sillmann, J., Kharin, V. V., Zhang, X., Zwiers, F. W., & Bronaugh, D. (2013). Climate extremes indices in the CMIP5 multimodel ensemble: Part 1. Model evaluation in the present climate. *Journal of Geophysical Research: Atmospheres*, 118, 1716–1733. <https://doi.org/10.1002/jgrd.50203>
- Smid, M., Russo, S., Costa, A. C., Granell, C., & Pebesma, E. (2019). Ranking European capitals by exposure to heat waves and cold waves. *Urban Climate*, 27, 388–402. <https://doi.org/10.1016/J.UCLIM.2018.12.010>
- Thompson, V., et al. (2022). The 2021 western North America heat wave among the most extreme events ever recorded globally. *Science Advances*, 8, eabm6860.
- Thompson, V., Mitchell, D., Hegerl, G. C., et al. (2023). The most at-risk regions in the world for high-impact heatwaves. *Nature Communications*, 14, 2152. <https://doi.org/10.1038/s41467-023-37554-1>
- Tomczyk, A. M., Pórolniczak, M., & Bednorz, E. (2017). Circulation conditions' effect on the occurrence of heat waves in Western and Southwestern Europe. *Atmosphere*, 8(2), 31. <https://doi.org/10.3390/atmos8020031>
- Yazdanpanah, H., Eitzinger, J., & Baldi, M. (2017). Analysis of the extreme heat events in Iran. *International Journal of Climate Change Strategies and Management*, 9(4), 418-432.
- Zhao, Q., Li, S., Ye, T., Wu, Y., Gasparrini, A., Tong, S., et al. (2024). Global, regional, and national burden of heatwave-related mortality from 1990 to 2019: A three-stage modelling study. *PLoS Medicine*, 21(5), e1004364. <https://doi.org/10.1371/journal.pmed.1004364>

Supplementary A:

Modeling the Sum of Three-Day Maximum Temperatures Using Pearson Type III Distribution: Methodology and Goodness-of-Fit Analysis

This analysis treats the sum of three-day maximum temperatures exceeding the 90th percentile as a random variable X . To model this, we employed the Pearson Type III probability function, characterized by the following probability density function:

$$f(x) = \frac{1}{b \cdot \Gamma(k)} \left(\frac{x-a}{b}\right)^{k-1} e^{-\left(\frac{x-a}{b}\right)} \quad (2)$$

where a is the mean of the distribution, b is the standard deviation, k is the shape parameter of the distribution, and $\Gamma(k)$ is the gamma function.

To estimate the three parameters of the above probability function, the following steps were performed:

- First, the skewness coefficient of the annual maximum data was calculated as the random variable X .
- Next, if the skewness of the data was positive (negative), the absolute minimum (maximum) of the observations was calculated, and the absolute maximum was designated as the extremum.
- Then, the new random variable “ X_{extremum} ” was calculated in the case of positive skewness, and “ $\text{extremum}-X$ ” in the case of negative skewness, and was named “ X ”.
- Subsequently, q was calculated as the percentage of occurrences of the number zero in the series “ X ”, including at least one case.
- Next, the auxiliary variable $A = \ln(\overline{X'}) - \overline{\ln(X')}$ was calculated.

- The initial estimate of the shape parameter of the Pearson Type III function was set to $\kappa = \frac{1}{4A} \left(1 + \sqrt{1 + \frac{4A}{3}} \right)$ and the initial estimate of the scale parameter $b = \frac{\bar{X}'}{\kappa}$ with the initial guess for the location parameter a) set close to zero.
- Using the initial parameter estimates in step 6 and applying the inverse cumulative probability function or the corresponding quantile function, a new estimate for the location parameter a was calculated.
- By defining the new random variable $X'' = X' + a$, steps 5 and 6 were repeated.
- Then, the values of X were sorted in ascending order, and the empirical Weibull probability function was calculated using the definition $P = \frac{m}{n-1}$ (where m is the rank of each observation in the ordered series and n is the total number of observations, i.e., the number of years in which at least one heat wave occurred). By applying the quantile function of the Pearson Type III distribution, the corresponding values for the observations were extracted and named $X_{pearson}$.
- Using the normal probability function with a scale parameter equal to the standard deviation of the observations and a location parameter equal to the mean of the observations, the corresponding quantile function was similarly calculated as X_{normal} .
- By calculating the sum of squared errors $\sum ((X - X_{pearson})^2)$ and $\sum ((X - X_{normal})^2)$, the smallest value was considered as an indicator of the goodness of fit for the mentioned probability function. It is important to note that in practice, if the absolute value of the skewness of the observations X is not greater than 0.35, in most cases, the normal probability function will yield a more realistic result in the goodness-of-fit test.